RSC Advances

PAPER

View Article Online
View Journal | View Issue

Cite this: *RSC Adv.*, 2017, **7**, 53290

Understanding the temperature–resistance performance of a borate cross-linked hydroxypropyl guar gum fracturing fluid based on a facile evaluation method†

Haiming Fan, *[ab] Zheng Gong,[a] Zhiyi Wei,[a] Haolin Chen,[a] Haijian Fan,[a] Jie Geng,[a] Wanli Kang [a] and Caili Dai[a]

The evaluation of the temperature–resistance performance of fracturing fluid is essential for choosing suitable fracturing fluids during fracturing treatment. In this work, related parameters for characterizing the temperature–resistance performance of fracturing fluids have been analysed systematically. The maximum temperature, $T_{max}(\eta_0, t_0)$, which satisfies both the minimum viscosity requirement ($\eta \geq \eta_0$) of fracturing fluid and the time requirement of fracturing treatment ($t \geq t_0$), was used to characterize the temperature–resistance performance of fracturing fluids. A facile procedure for evaluating $T_{max}(\eta_0, t_0)$ has been proposed based on a step-by-step numerical-search method. The search for $T_{max}(\eta_0, t_0)$ starts from the upper limit temperature T_{max}, which is the maximum temperature where the apparent viscosity meets the minimum viscosity requirement, *i.e.*, $\eta \geq \eta_0$. Using a borate cross-linked hydroxypropyl guar gum fracturing fluid as an example, the effects of pH, and the concentrations of thickening agent (hydroxypropyl guar, HPG) and crosslinking agent ($Na_2B_4O_7$) on the crosslink and temperature–resistance properties are also investigated. It has been found that the crosslinking time t_c decreases with the increase of HPG concentration or $Na_2B_4O_7$ concentration. However, t_c was found to increase when pH increases. The variation tendencies of $T_{max}(\eta_0, t_0)$ are different from that of T_{max}, *viz.*, $T_{max}(\eta_0, t_0)$ gradually increases with $Na_2B_4O_7$ concentration, whereas T_{max} increases significantly at low $Na_2B_4O_7$ concentration and remains almost unchanged at high $Na_2B_4O_7$ concentration. The possible mechanisms are proposed for interpreting the above phenomena according to related crosslinking-reaction kinetics and thermodynamics. Our work demonstrates a facile method for evaluating the temperature–resistance performance of the fracturing fluid and provides useful insights into the understanding of the temperature tolerance performance of the borate cross-linked hydroxypropyl guar gum fracturing fluid.

Received 23rd October 2017
Accepted 14th November 2017

DOI: 10.1039/c7ra11687j

rsc.li/rsc-advances

1. Introduction

Hydraulic fracturing is a commonly used technique to stimulate hydrocarbon production by creating a network of highly conductive fractures in the area surrounding a wellbore.[1] The network of fractures can not only improve the hydraulic conductivity of the reservoir rock, but also increase the surface area contributing to enhanced hydrocarbon production.[1,2] Thus, hydraulic fracturing is used in conventional hydrocarbon reservoirs to increase permeability in damaged formations or in formations that exhibit significantly lower production owing to reservoir depletion. It is also used in unconventional reservoirs where the intrinsic permeability is too low to yield economical production.[3–5] Fracturing fluid is of great significance for hydraulic fracturing treatment. The main functions of fracturing fluid include opening the fracture, and suspending and transporting proppants.[1] So, a fracturing fluid is supposed to provide sufficient viscosity to ensure proper proppant transport and the even distribution of proppants along the fractures. Over the past few decades, linear or cross-linked polymer solutions,[6–9] energized fluids,[10–12] and viscoelastic surfactants (VES)[13–18] have been developed as water-based fracturing fluids. Biopolymers such as guar gum and cellulose derivatives, synthetic polymers such as polyacrylamide, are introduced in the water-based fracturing fluids for improving the rheological performance.[2] Crosslinking improves the rheological properties of the polymers for fracturing purposes, *e.g.* borate, Ti(IV), Zr(IV), and Al(III) ions are often used to crosslink water soluble polymers.[19–21] Guar gum and its derivatives, such as hydroxypropyl

[a]*Shandong Provincial Key Laboratory of Oilfield Chemistry, School of Petroleum Engineering, China University of Petroleum (East China), Qingdao 266580, Shandong Province, P. R. China. E-mail: haimingfan@126.com*

[b]*State Key Laboratory of Oil and Gas Reservoir Geology and Exploitation, Southwest Petroleum University, Chengdu 610500, Sichuan Province, P. R. China*

† Electronic supplementary information (ESI) available. See DOI: 10.1039/c7ra11687j

guar (HPG), carboxymethyl guar (CMG) and carboxymethyl hydroxypropyl guar (CMHPG), are the most-common polymers used in fracturing fluid, accounting for up to 90% of all gelled fracturing fluids.[1,22] Meanwhile, to satisfy the criterion to fracture deeper and hotter wells, synthetic terpolymer of 2-acrylamido-2-methylpropanesulfonic acid (AMPS), acrylamide and acrylate cross-linked by Zr has been developed and used as a fracturing fluid.[23,24]

The evaluation on the temperature–resistance performance of fracturing fluid is essential for choosing the suitable fracturing fluid with excellent performance. Generally, two main methods were used to evaluate the temperature–resistance performance of fracturing fluid.[25–35] One is to monitor the changes of the apparent viscosity at a constant shear rate with increasing temperature by continuously heating the fracturing fluid.[25–27] The apparent viscosity decreases with increasing temperature and when it drops to a certain value, the indicated temperature is used as the thermal stability temperature of fracturing fluid. For example, Baruah *et al.* found that the VES fracturing fluid developed from Tween 80/NaOA/2-ethyl hexanol/clove oil/water system presented an apparent viscosity at shear rate 100 s^{-1} greater than 90 mPa s when the temperature is below 116.3 °C. The insertion of 500 ppm ZnO nanoparticle further improved the thermal stability temperature to 119.5 °C.[25] The other method is to measure the changes of the apparent viscosity with time under constant temperature. Generally, the temperature–resistance performance of the fracturing fluid is obtained by either analysing the apparent viscosity after heating or measuring the stability time when the apparent viscosity of the fluid is above criterion value at different temperatures.[28–35] For example, Holtsclaw *et al.* measured the apparent viscosity of zirconium cross-linked terpolymer gel as a function of time at 177, 191, 204 and 218 °C. It is found that the apparent viscosity at shear rate 40 s^{-1} of the gel was greater than 2000 mPa s after shearing for 4 hours at 177 °C, almost 500 mPa s after shearing for 4 hours at 204 °C, and approximately 300 mPa s after shearing for 2 hours at 218 °C.[29] So they concluded the synthetic zirconium cross-linked terpolymer gel with good stability at temperature larger than 177 °C. Wang *et al.* found that the apparent viscosity of organic zirconium cross-linked terpolymer gel can reach 130 mPa s after 90 min of shearing at shear rate 170 s^{-1} at 220 °C, and but it is concluded that the fracturing fluid resists at high temperature of 220 °C.[35]

The duration time when the viscosity of fracturing fluid meets the required apparent viscosity for fracturing at the formation temperature should be larger than the time of fracturing treatment.[1] Otherwise, it will affect the efficiency of fracturing fluid during fracturing treatment. Consequently, when evaluating the temperature–resistance performance of fracturing fluid, not only the required apparent viscosity, but also the duration time should be considered. For this reason, the second evaluation method is used more often. However, most of previous tests are not conducted under uniform standard conditions, *e.g.* the measurement of apparent viscosity is not at a same shear rate, so the apparent viscosities have to be measured and compared again when developed new thickening agent, crosslinking agent and other chemical additive agents. Furthermore, so far as we know, there is no evaluation method for accurately determining the maximum tolerance temperature of the fracturing fluid, which leads to the fact that the effectiveness of temperature stabilizer and chelating agent can only be indirectly reflected by measuring the apparent viscosity changes of the fracturing fluid at a certain temperature.[36,37] Thus, it is still necessary to explore a standard method on evaluating the temperature–resistance performance of fracturing fluid, which will remarkably benefit researchers and users for the screening and developing of fracturing fluids.

The key point of the evaluation on the temperature–resistance performance of fracturing fluid is to establish a method for measuring the maximum tolerance temperature which meets the criteria for the apparent viscosity and the time requirement of the fracturing treatment. Our previous work demonstrated a way of evaluating the effectiveness of temperature stabilizer by measuring the difference of the maximum tolerance temperature in satisfying the criteria of fracturing treatment before and after adding the temperature stabilizer.[38] However, no systematic study on the influence of main components in fracturing fluid on the temperature resistance performance has been published yet. Herein, in this work, related parameters for characterizing the temperature–resistance performance of fracturing fluid have been analysed. And the maximum tolerance temperature is determined by a step-by-step numerical search method starting from the upper limit temperature. By using this method, influence factors such as pH, the concentration of thickening agent (*e.g.*, HPG) and crosslinking agent (*e.g.*, $Na_2B_4O_7$) on the crosslink and temperature–resistance properties of borate cross-linked hydroxypropyl guar gum fracturing fluid are investigated and the influence mechanisms are also discussed.

2. Materials and methods

2.1. Materials

Hydroxypropyl guar gum with an average molecular weight of 3.2×10^6 Da is commercially available and supplied by Shandong Dongying Xinde Chemical Co., Ltd. Borax ($Na_2B_4O_7 \cdot 10H_2O$, 99%) and sodium hydroxide (NaOH, 99%) are all A.R. grade and from Beijing Chemical Company. The water was triply distilled by a quartz water purification system. All reagents are used without further treatment.

2.2. Sample preparation

The desired amount of HPG is added to the water in a 500 ml beaker and stirred at 6000 rpm for 5 min. Then 5 wt% NaOH is added dropwise to adjust the pH to desired value. These HPG solutions are continuously stirred for 5 min and sealed in a 30 °C thermostatic bath for above 4 hours, which is used as the base fluid for the preparation of fracturing fluid. The base liquid is added and stirred at 300 rpm in a 250 ml beaker. After the addition of the desired amount of cross-linked agent $Na_2B_4O_7$, the mixture is continuously stirred to form a uniform fracturing fluid system. The fracturing fluid is then sealed in

a 30 °C thermostatic bath for more than 6 hours before rheology measurements.

2.3. Crosslinking time measurements

The crosslinking time of the borate cross-linked hydroxypropyl guar gum fracturing fluid is measured by macroscopic appearance observation at 30 °C. Typically, 100 ml base liquid is added and stirred at 300 rpm in a 250 ml beaker, and the desired amount of borate is added to the base liquid. Continue stirring until the vortex disappears and the liquid surface has just risen, and the time is defined as the crosslinking time.

2.4. Rheology measurements

The rheological properties of samples are measured with a high temperature and high pressure rheometer (HAAKE MARS-III, Thermo Fisher Scientific). For measuring the viscosity–temperature curve of the fracturing fluid, the sample was continuously sheared at the shear rate of 170 s^{-1} and heated at the rate of 3.0 ± 0.2 °C min^{-1}, and then the apparent viscosity was measured at the corresponding temperature. For measuring the viscosity–time curve of the fracturing fluid, the sample was continuously sheared at the shear rate of 170 s^{-1} and heated to the setting temperature. Then the apparent viscosity was measured as a function of time.

3. Evaluation method for the temperature–resistance performance

3.1. Temperature–resistance performance of fracturing fluid

Table 1 shows the parameters for characterizing the temperature–resistance performance of fracturing fluid according to the technical requirement of fracturing treatment. η_0, t_0 and T_0 are the minimum viscosity requirement of fracturing fluid, time requirement and formation temperature for fracturing treatment, respectively. And η is the apparent viscosity of fracturing fluid at a certain shear rate. The two temperatures, *viz.*, T_{max} and $T_{max}(\eta_0, t_0)$ and the duration time $t(T)$ are the most important parameters to characterize the thermal stability of the fracturing fluid. Firstly, T_{max} is the maximum temperature where the apparent viscosity meets the minimum viscosity requirement of fracturing fluid, and T_{max} is also the highest temperature to satisfy the condition of $\eta[T] \geq \eta_0$. A convenient way to determine T_{max} is through measuring the apparent viscosity as a function of temperature. Normally, the apparent viscosity decreases with increasing temperature and when it drops to η_0, the corresponding temperature is defined as T_{max}. Secondly, $t(T)$ is the duration time where the apparent viscosity meets the minimum viscosity requirement of fracturing fluid at temperature T, and $t(T)$ is also the longest time to satisfy the condition of $\eta[T, t] \geq \eta_0$. The way to determine $t(T)$ is by measuring the apparent viscosity as a function of time at temperature T. And the difference between the time when η drops to η_0 and the time when the temperature rises to the setting temperature is defined as $t(T)$. Thirdly, $T_{max}(\eta_0, t_0)$ is the maximum temperature where the apparent viscosity meets both the minimum viscosity requirement of fracturing fluid and the duration time requirement of fracturing treatment. In other words, $T_{max}(\eta_0, t_0)$ is also the highest temperature to satisfy the condition $\eta[T, t_0] \geq \eta_0$. It can be experimentally determined by measuring the $t(T)$ of fracturing fluid at several temperatures, and $T_{max}(\eta_0, t_0)$ is the highest temperature to satisfy the condition $t(T) \geq t_0$. Furthermore, it is worth noting that T_{max} is always larger than $T_{max}(\eta_0, t_0)$ because of the degradation of fracturing fluid accompanied by a decrease in apparent viscosity with the increase of heating time.

The condition for fracturing fluids to meet the requirements for fracturing treatment is $\eta[T_0, t \geq t_0] \geq \eta_0$, which means that at the formation temperature T_0, the duration time $t(T_0)$ shall be larger than the time requirement for fracturing treatment t_0. Thus, once t_0, η_0 and T_0 are determined in the designed fracturing project, there are three possible situations according to the relationship between T_{max}, $T_{max}(\eta_0, t_0)$ and T_0. When $T_0 \leq T_{max}(\eta_0, t_0)$, the temperature–resistance performance of

Table 1 Related parameters for characterizing the temperature resistance performance of fracturing fluid

Symbol	Physical meaning	Mathematical expression
η_0	Minimum viscosity requirement of fracturing fluid for fracturing treatment	
t_0	Time requirement for fracturing treatment	
T_0	Formation temperature for fracturing treatment	
η	Apparent viscosity of fracturing fluid at a certain shear rate	
T_{max}	Maximum temperature where the apparent viscosity meets the minimum viscosity requirement of fracturing fluid	$\eta[T] \geq \eta_0$ $\eta[T_{max}] = \eta_0$
$t(T)$	Duration time when the apparent viscosity meets the minimum viscosity requirement of fracturing fluid at temperature T	$\eta[T, t] \geq \eta_0$ $\eta[T, t(T)] = \eta_0$
$T_{max}(\eta_0, t_0)$	Maximum temperature where the apparent viscosity meets the minimum viscosity requirement of fracturing fluid and the duration time meets the time requirement of fracturing treatment	$\eta[T, t_0] \geq \eta_0$ $\eta[T_{max}(\eta_0, t_0), t_0] = \eta_0$

fracturing fluid can satisfy the requirements of fracturing treatment. When $T_{max}(\eta_0, t_0) < T_0 \leq T_{max}$, the fracturing fluid cannot meet the treatment requirements, but the initial apparent viscosity is larger than η_0. Therefore, it is possible to consider delaying the reduction of viscosity by adding additives such as temperature stabilizer to meet the treatment requirements. When $T_0 > T_{max}$, the fracturing fluid has a low initial apparent viscosity thus it cannot meet the treatment requirements. So it is necessary to change the main-component concentration or the type of fracturing fluid to increase the thickening ability of fracturing fluid.

3.2. Evaluation procedure

Based on the above analysis, it can be seen that $T_{max}(\eta_0, t_0)$ is the parameter that directly reflects the temperature–resistance performance of the fracturing fluid in principle. Therefore, the key point for the evaluation method is to skilfully design experiments to determine $T_{max}(\eta_0, t_0)$ and avoid the boundless search. Owing to $T_{max} > T_{max}(\eta_0, t_0)$, the $T_{max}(\eta_0, t_0)$ can be determined by a step-by-step numerical search method starting from the upper limit temperature T_{max}, where the T_{max} is easily determined by measuring the viscosity–temperature curve. Inspired by this idea, we designed a facile method on evaluating the temperature–resistance performance of the fracturing fluid and the specific experimental procedures are brief illustrated and shown in Fig. 1, and this method mainly includes the following steps.

(1) Setup the minimum viscosity requirement of fracturing fluid η_0 and the time requirement t_0 based on the requirements for fracturing treatment.

(2) Determination of T_{max} by measuring the viscosity–temperature curve of fracturing fluid.

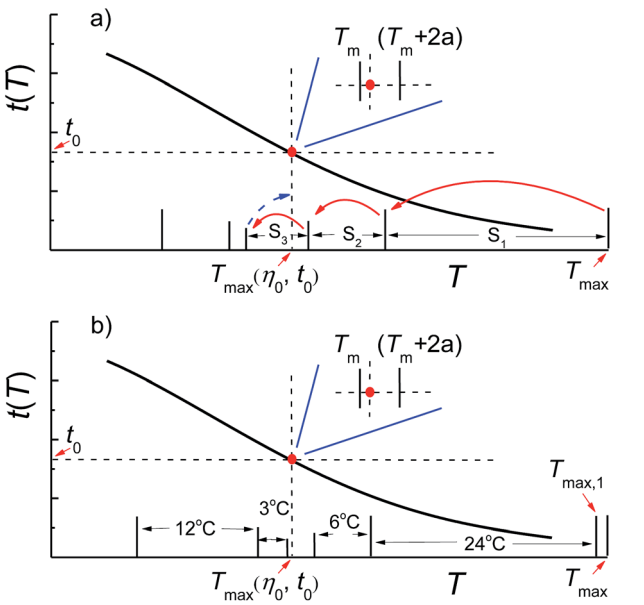

Fig. 1 Scheme for determining the $T_{max}(\eta_0, t_0)$ of fracturing fluid by one-dimensional numerical search method. (a) Random numerical search method; (b) binary search method.

(3) Determination of $T_{max}(\eta_0, t_0)$ by numerical search method (Fig. 1a):

(i) Setup the initial search length S_0 and the precision k of the numerical search;

(ii) Measure the $t(T)$ of the fracturing fluid at $(T_{max} - S_0 \times n)$ °C, where n is a natural number. The test was stopped when $t(T) \geq t_0$, and the current temperature was recorded as $T(t)$;

(iii) If $t(T) = t_0$, stop search and execute step (vi); if $t(T) > t_0$, order $T(t) = T_m$, where m is the number of times for execution steps (ii) and (iii), execute step (iv) until the step (v) is satisfied and then execute step (vi);

(iv) Shorten the search length to S_m and repeat steps (ii) and (iii) at $(T_m + S_{m-1} - S_m \times n)$ °C in the temperature range of $T_m \sim T_m + S_{m-1}$;

(v) Order $a \leq k$, the measurement has been completed of $t(T_m)$ and $t(T_m + 2a)$, and meanwhile, the condition of $t(T_m) > t_0$ and $t(T_m + 2a) < t_0$ is also satisfied;

(vi) If $t(T) = t_0$, the current $T(t)$ is $T_{max}(\eta_0, t_0)$ that conforms to the precision of numerical search; if $t(T_m) > t_0$ and $t(T_m + 2a) < t_0$, the $(T_m + a)$ is $T_{max}(\eta_0, t_0)$ that conforms to the precision of numerical search.

It is noted that the rigorous mathematical formulation is given in the above evaluation method. However, there are still many experimental steps that can be carried out flexibly. Firstly, the upper limit temperature $T_{max,1}$ can be chose near T_{max}, satisfying the condition of $t(T_{max,1}) < t_0$. This will facilitate the subsequent temperature setting in the test, because T_{max} may be a fraction depending on the preset heating rate in the viscosity–temperature curves measurement. Secondly, the binary search method is recommended as the numerical search method. Although the golden section method, Fibonacci method and other one-dimensional numerical search method are better strategy compared to the binary search method, but the programs are relatively complex and difficult to master.[39,40] In the binary search method, the step length of numerical search is reduced by half during each step, which is easy to master. Fig. 1b shows the scheme of binary search method where $T_{max,1}$ is the upper limit temperature and 24 °C is the initial search length.

In order to further explain the determination of the specific parameters in the designed evaluation method, the fracturing fluid prepared by 0.3 wt% HPG/0.8 wt% $Na_2B_4O_7$ cross-linked at pH 9 is chosen to investigate the temperature resistance performance. Since the prepared fracturing fluid is a water-based gelling fracturing fluid, the minimum viscosity requirement of fracturing fluid η_0 and the time requirement t_0 are set as 50 mPa s and 120 min, respectively, and the apparent viscosity is measured at shear rate 170 s^{-1} according to the general technical specifications of fracturing fluid in China.[41] Fig. 2 shows the viscosity–temperature curve of the fracturing fluid. It can be seen that the T_{max} of the fracturing fluid is 104.9 °C. And then the upper limit temperature $T_{max,1}$, the initial search length S_0 and the precision k for the binary search method are set as 105 °C, 24 °C and 0.5 °C, respectively. When the temperature is reduced by 24 °C from $T_{max,1}$ to

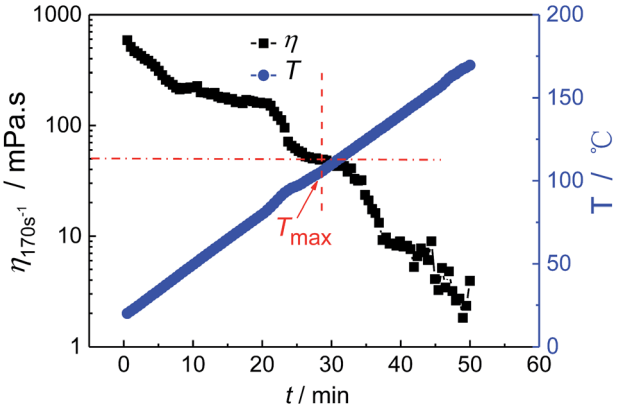

Fig. 2 The viscosity–temperature curve of the fracturing fluid. The fracturing fluid is prepared by 0.3 wt% HPG/0.8 wt% $Na_2B_4O_7$ cross-linked at pH = 9.

81 °C, the temperature reaches the set point after 12 min heating, and the apparent viscosity is greater than 50 mPa s within the overall test time of 150 min (Fig. 3a). It is indicated that the $t(T = 81\ °C)$ of the fracturing fluid is larger than 138 min, which is higher than 120 min. Thus, the $T_{max}(\eta_0, t_0)$ of the fracturing fluid is between 81 °C and 105 °C. Fig. 3b shows the viscosity–time curve at 93 °C, and the $t(T = 93\ °C)$ is 31 min by calculating the difference between the time when η drops to η_0 and the time when the temperature is raised to the setting temperature, which further limits the search range to 81–93 °C. Similarly, the viscosity–time curves of the fracturing fluid at 87 °C, 90 °C, 88 °C, 89 °C are also measured in turn and were shown in Fig. 3c–f. It is observed that the $t(T = 88\ °C)$ and $t(T = 89\ °C)$ satisfied the condition of $t(T = 88\ °C) > 120$ min and $t(T = 89\ °C) < 120$ min and the $T_{max}(\eta_0, t_0)$ is 88.5 °C which conforms to the preset precision of this numerical search method.

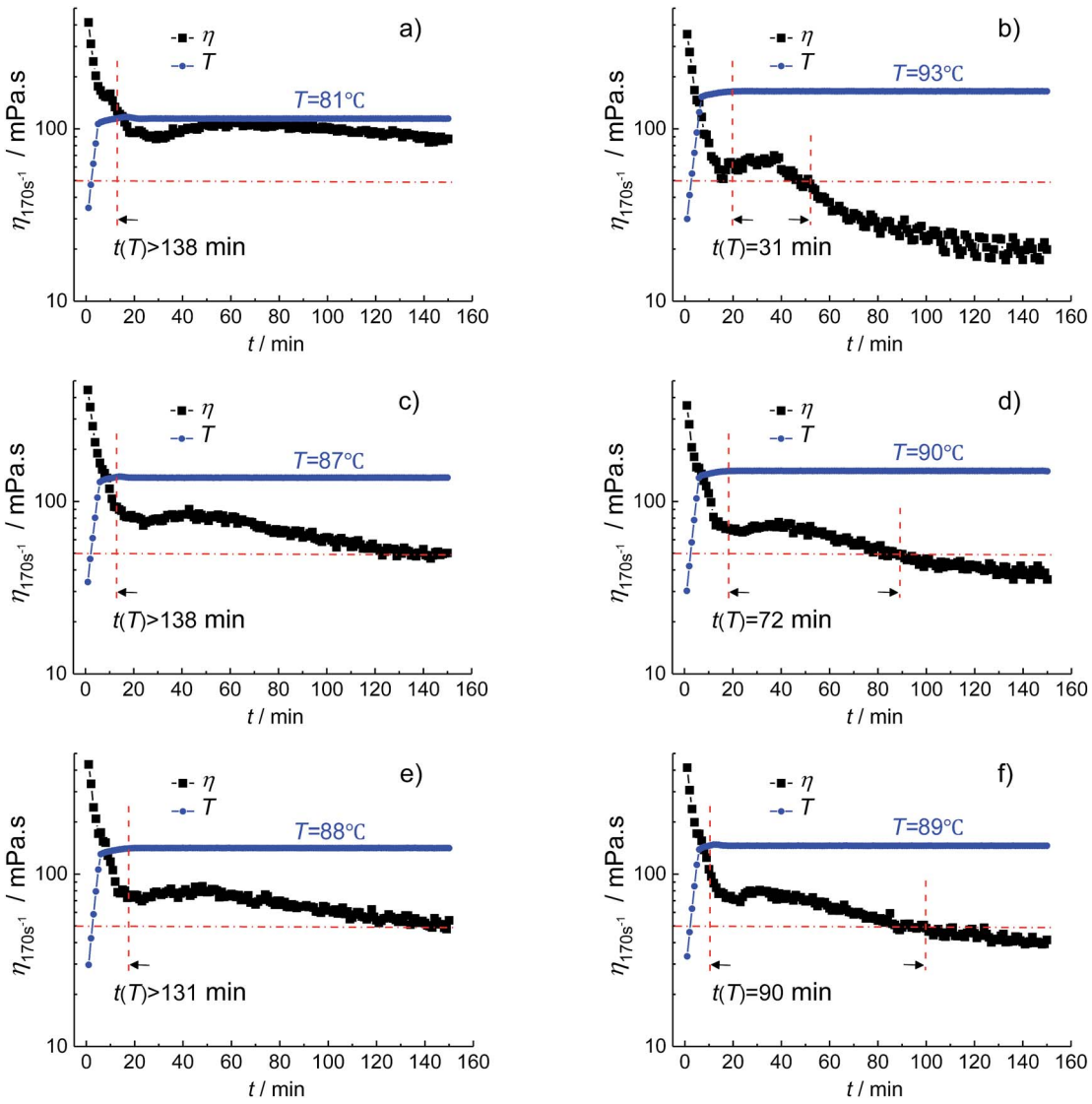

Fig. 3 The viscosity–time curves of the fracturing fluid at different temperature. The fracturing fluid is prepared by 0.3 wt% HPG/0.8 wt% $Na_2B_4O_7$ cross-linked at pH = 9.

4. Influencing factors and mechanisms on the temperature–resistance performance

4.1. Influencing factors

The polymer concentration is a key factor affecting the structure and properties of cross-linked gel fracturing fluid system. Fig. 4 shows the effect of HPG concentration W_{HPG} on the crosslinking time t_c, T_{max} and $T_{max}(\eta_0, t_0)$. It can be seen from Fig. 4a that the crosslinking time t_c is 480 s when the HPG concentration is 0.2 wt%. The crosslinking time t_c will decrease with the increasing of HPG concentration and t_c reaches 25 s when the HPG concentration is 0.8 wt%. Considering that the friction is too large at the initial stage of fracturing if the crosslinking is too fast, the HPG concentration isn't further increased in the cross-linked gel fracturing fluid. The experiment results on the evaluation of the temperature–resistance performance of the fracturing fluid at different HPG concentrations are shown in Fig. S1–S7 and Tables S1–S7 at the ESI.† And the effect of HPG concentration on T_{max} and $T_{max}(\eta_0, t_0)$ are summarized in Fig. 4b. It can be seen that the T_{max} and $T_{max}(\eta_0, t_0)$ of the fracturing fluid all increase with the HPG concentration. The T_{max} and $T_{max}(\eta_0, t_0)$ are 51.1 °C and 39 °C when the HPG concentration is 0.2 wt%. When the concentration of HPG increased to 0.45 wt%, the T_{max} and $T_{max}(\eta_0, t_0)$ are 150.9 °C and 99.5 °C, respectively, which increase by 99.8 °C and 60.5 °C as compared to those at 0.2 wt% HPG. Further increasing the concentration of HPG to 0.8 wt% will result in the increase of T_{max} for 16.4 °C to 167.3 °C, whereas the $T_{max}(\eta_0, t_0)$ has gone up 34 °C to 133.5 °C compared to those at 0.45 wt% HPG.

Another influencing factor on the crosslink and temperature–resistance properties of the fracturing fluid is the concentration of crosslinking agent. Fig. 5 shows the plots of the crosslinking time t_c, T_{max} and $T_{max}(\eta_0, t_0)$ as a function of $Na_2B_4O_7$ concentration, W_C, respectively. It can be seen from Fig. 5a that the crosslinking time t_c decreases with the increase of $Na_2B_4O_7$ concentration. And the crosslinking time t_c is 720 s and 30 s for 0.2 wt% $Na_2B_4O_7$ and 2.0 wt% $Na_2B_4O_7$, respectively. The experiment results on the evaluation of the temperature–resistance performance of the fracturing fluid at different $Na_2B_4O_7$ concentrations are shown in Fig. S8–S18 and Tables S8–S18 at the ESI.† And the effect of $Na_2B_4O_7$ concentration on T_{max} and $T_{max}(\eta_0, t_0)$ are summarized in Fig. 5b. It can be seen that both T_{max} and $T_{max}(\eta_0, t_0)$ of the fracturing fluid increase

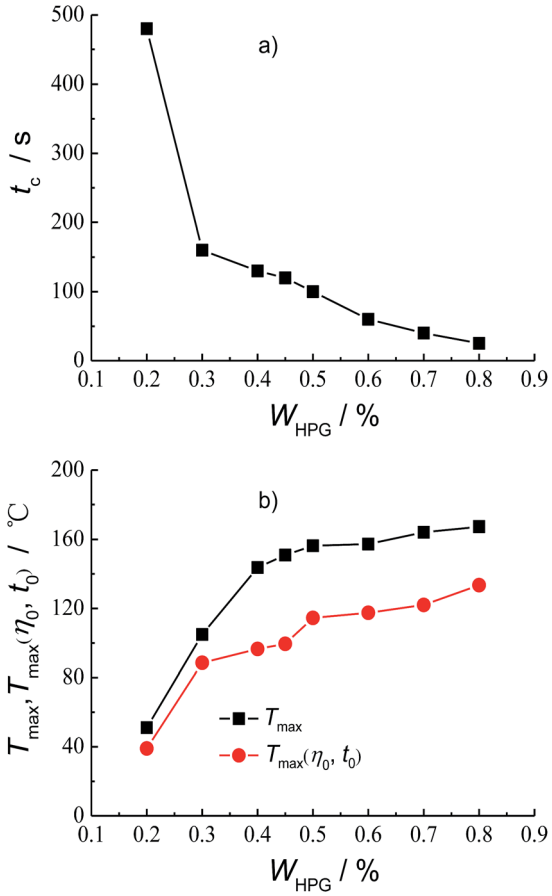

Fig. 4 (a) The crosslinking time t_c, (b) T_{max} and $T_{max}(\eta_0, t_0)$ as a function of HPG concentration (W_{HPG}) of the fracturing fluid. The fracturing fluid is prepared by HPG/0.8 wt% $Na_2B_4O_7$ cross-linked at pH = 9.

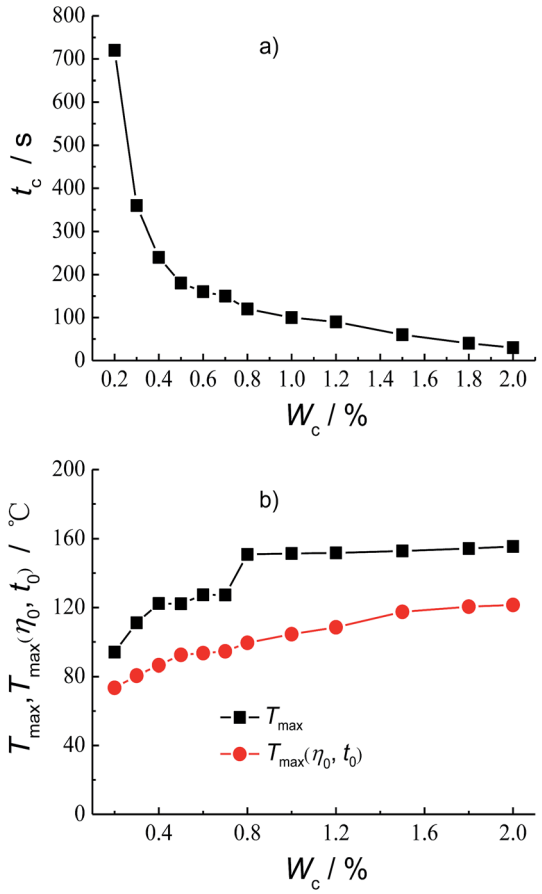

Fig. 5 (a) The crosslinking time t_c, (b) T_{max} and $T_{max}(\eta_0, t_0)$ as a function of crosslinking agent concentration (W_C) of the fracturing fluid. The fracturing fluid is prepared by 0.45 wt% HPG/$Na_2B_4O_7$ cross-linked at pH = 9.

with $Na_2B_4O_7$ concentration, but the variation tendencies are different. Within the concentration range of 0.2–0.8 wt%, T_{max} increases by 56.8 °C, whereas in the concentration range from 0.8 wt% to 2.0 wt%, T_{max} only increases by 4.6 °C. In comparison, $T_{max}(\eta_0, t_0)$ gradually increases with the increase of $Na_2B_4O_7$ concentration, *e.g.* $T_{max}(\eta_0, t_0)$ increases by 26 °C when the $Na_2B_4O_7$ concentration changed from 0.2 wt% to 0.8 wt%, meanwhile, the $T_{max}(\eta_0, t_0)$ increases by 22 °C when the $Na_2B_4O_7$ concentration increases from 0.8 wt% to 2.0 wt%.

The pH when the crosslinking reaction occurs also affects the properties of fracturing fluid. Fig. 6 shows the effect of pH on the crosslinking time t_c, T_{max} and $T_{max}(\eta_0, t_0)$. It can be seen from Fig. 6a that the crosslinking time increases with the increase of pH. The crosslinking time t_c is 40 s at pH 7 and 220 s at pH 13. The experiment results on the evaluation of the temperature resistance performance of the fracturing fluid at different pH are shown in Fig. S19–S24 and Tables S19–S24 at the ESI.† And the effect of pH on T_{max} and $T_{max}(\eta_0, t_0)$ are summarized in Fig. 6b. It can be seen that the T_{max} increases from 98.7 °C to 159.3 °C when the pH increases from 7 to 11. And then the T_{max} gradually decreases after reaching the maximum. The T_{max} reduced to 150.8 °C when the pH goes up from 11 to 13. The $T_{max}(\eta_0, t_0)$ increases from 77.5 °C to 99.5 °C with the pH rising from 7 to 9. However, the $T_{max}(\eta_0, t_0)$ almost unchanged in the pH range from 9 to 11. When the pH increases to 13, the $T_{max}(\eta_0, t_0)$ continually increases to 116.5 °C and increases by 17 °C compared with that at pH 11.

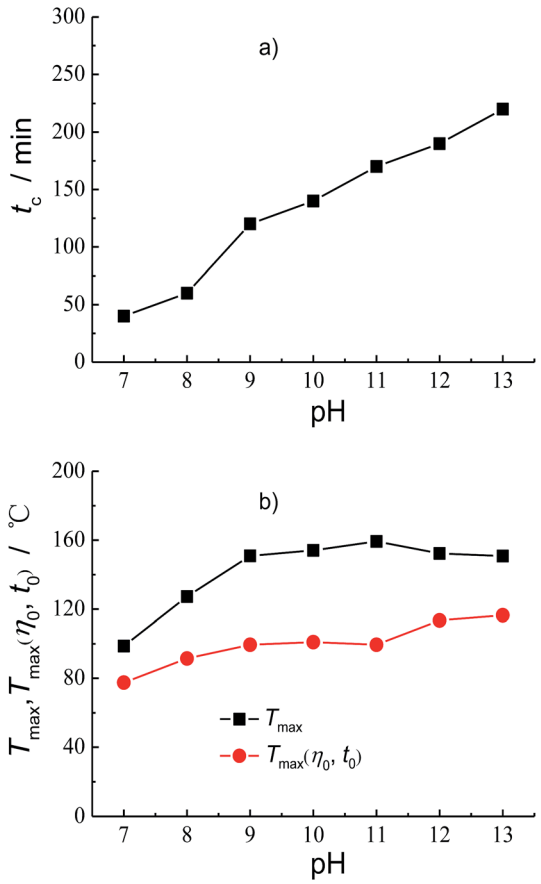

Fig. 6 (a) The crosslinking time t_c, (b) T_{max} and $T_{max}(\eta_0, t_0)$ as a function of pH of the fracturing fluid. The fracturing fluid is prepared by 0.45 wt% HPG/0.8 wt% $Na_2B_4O_7$ cross-linked at different pH.

4.2. Influencing mechanisms

Through the designed evaluation method, the crosslink and temperature–resistance properties of $Na_2B_4O_7$ cross-linked HPG fracturing fluid are studied in detail. It is interesting to analysis and discuss the dependence of t_c, T_{max} and $T_{max}(\eta_0, t_0)$ on the HPG concentration, the $Na_2B_4O_7$ concentration and the pH. It is helpful to further clarify the relationship between the measured parameters and gel properties. Firstly, the crosslinking time t_c reflects the rate at which the crosslinking of fracturing fluid reaches the gel state. This definition is proposed from the viewpoint of fracturing treatment. If the gel state is achieved, the friction of fracturing fluid in the initial injection process will be remarkably increased.[42] It is worth noting that the gel forms in a short time when HPG mixed with $Na_2B_4O_7$ as shown in Fig. 4a, 5a and 6a. However, the crosslinking reaction is still in progress with time and the gel properties such as strength are also changing. The time when the gel reaches thermodynamic equilibrium (*e.g.*, strength does not change) is called gelation time. Experimental results indicated by Rietjens *et al.* show the gelation time could go up to 750–22 000 s when the pH changes from 10.6 to 12.85 for the borate cross-linked HPG fracturing fluid.[43] That is why the prepared fracturing fluids are sealed for above 6 hours in this study to obtain the relatively stable gel for evaluating the temperature–resistance performance. Secondly, it can be seen from Table 1, the measured T_{max} is the maximum temperature where the apparent viscosity meets the minimum viscosity requirement of fracturing fluid. Thus, the T_{max} reflects the viscosifying ability, which is closely related to the molecular weight and distribution of the crosslinking system of the fracturing fluid.[44] As the temperature increases, the molecular thermal motion increases in the cross-linked gel system, so the intermolecular distance in the cross-linked gel network increases, which induces the decreases of flow resistance as well as viscosity. Thirdly, the high temperature treatment of the cross-linked gel will lead to the gel degradation owing to the cleavage of crosslinking and chemical bond induced by thermal hydrolysis, the thermal oxidation and other decomposition pathways.[45–47] Because the gel degradation is a gradual process, the reduction of viscosity is highly related to the heating time, in other words, the longer the action time, the higher the degree of degradation and the more serious the viscosity decreases. Thus the measured $T_{max}(\eta_0, t_0)$ comprehensively reflects both the viscosifying ability and the degradation tolerance ability, which is not only closely related to the molecular weight and distribution of the crosslinking system, but also with the degradation process.

The *cis*-OH pairs on the galactose side chains in HPG molecules can undergo 1–1 and 2–1 crosslinking with borate and the 2–1 crosslinking reaction can be divided into intramolecular and intermolecular crosslinking as illustrated in Fig. 7.[2] These cross-linked structures are in dynamic equilibrium in solution. The intermolecular 2–1 crosslinking is

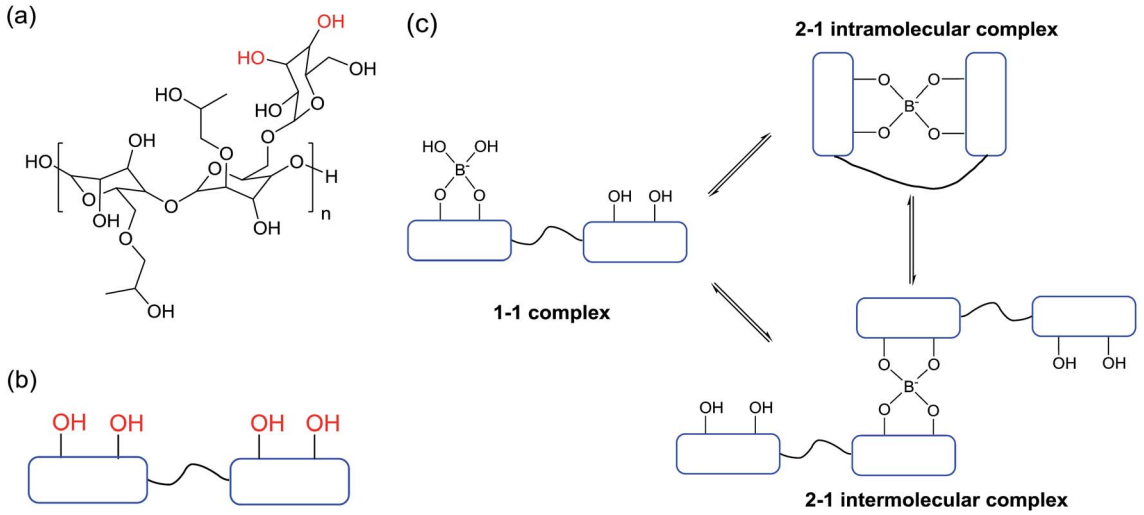

Fig. 7 The molecular structure of HPG (a), the simplified molecular structure of HPG (b) and the crosslinking reactions between borax and HPG (c).

effective for the formation of network structure, which significantly increases the molecular weight of the cross-linked gel system and the corresponding viscosity of the fracturing fluid (Fig. 7). With the increase of HPG concentration, more crosslinking sites will appear and higher chance of crosslinking reaction will happen. At the same time, the decrease of intermolecular distance between HPG is more favourable for intermolecular 2–1 crosslinking reaction. Thus, the rate of gelation increases, which leads to the decrease of crosslinking time t_c as observed in Fig. 4a. The degree of intermolecular 2–1 crosslinking increases, which makes the increase of the molecular weight of cross-linked gels, and thereby enhances the viscosity. Hence, the T_{max} of the cross-linked gel increase with the increase of HPG concentration (see Fig. 4b). When the concentration of crosslinking agent $Na_2B_4O_7$ is fixed, the crosslinking reaction will approach the upper limit of crosslinking degree accompanied by the increase of HPG concentration.[48,49] Although more crosslinking sites at high HPG concentration appears, the excess HPG molecules can only exist as non-cross-linked state. Therefore, in low concentration range (*e.g.*, 0.2–0.45 wt%), the increase of T_{max} value caused by the same amount of HPG is greater than that in the high concentration range (*e.g.*, 0.45–0.8 wt%) as shown in Fig. 4b. When the cross-linked gel degrades at high temperature, the non-cross-linked HPG molecules can react with the crosslinking agent $Na_2B_4O_7$ again. As a result, T_{max} changed slightly, but the $T_{max}(\eta_0, t_0)$ continued to increase in the high HPG concentration range (see Fig. 4b). However, once the cross-linked system degrades at low HPG concentration, the molecular weight of cross-linked gel would decrease significantly. Therefore, the enhancement of T_{max} is larger than that of $T_{max}(\eta_0, t_0)$ by adding the same amount of HPG in the low concentration range (*e.g.*, 0.2–0.45 wt%).

Similarly, when the concentration of thickening agent HPG is fixed, the rate of gelation increases and the crosslinking time t_c decreases with the increase of the $Na_2B_4O_7$ concentration (see Fig. 5a). Meanwhile, the increase of $Na_2B_4O_7$ concentration also promotes the intermolecular 2–1 crosslinking reaction, which results in the increase of the molecular weight and the viscosifying ability of cross-linked gels, and then the increase of T_{max}. However, the degree of crosslinking almost reaches maximum when the $Na_2B_4O_7$ concentration is above 0.8 wt%. So the molecular weight of cross-linked gel does not significantly increase by continue adding $Na_2B_4O_7$, where T_{max} behaves as almost a constant (see Fig. 5b). Meanwhile, those excessive $Na_2B_4O_7$ can crosslink again with low molecular weight HPG molecules produced by thermal degradation, which could result in the delayed degradation. Therefore, T_{max} remains unchanged but the $T_{max}(\eta_0, t_0)$ continues to increase after the $Na_2B_4O_7$ concentration was higher than 0.8 wt%. Whereas before reaching the maximum crosslinking degree, the change of T_{max} would be greater than that of $T_{max}(\eta_0, t_0)$ (Fig. 5b).

The crosslinking agent $Na_2B_4O_7$ will be hydrolyzed in aqueous solution to yield boric acid $B(OH)_3$ and borate anion $B(OH)_4^-$. The $B(OH)_3$ exists as a pH dependent equilibrium with the $B(OH)_4^-$ such that higher pH drives the reaction towards the formation of the $B(OH)_4^-$:

$$B(OH)_3 + H_2O = B(OH)_4^- + H^+$$

According to the experimental results of ^{11}B NMR spectra, both boric acid and borate ion have been implicated in the crosslinking step to form the 1–1 complex as shown in Fig. 8.[50] The 1–1 crosslinking reaction products will continue to undergo intramolecular or intermolecular 2–1 crosslinking reactions with HPG molecules. In the aspect of reaction kinetics, the reaction rate constant of a borate ion with *cis*-OH pairs is much smaller than that of boric acid.[51–55] Therefore, the crosslinking reaction slows down, and the crosslinking time increases with the increase of pH and the corresponding amount of borate ion (Fig. 6a). In the aspect of reaction thermodynamics, it has been

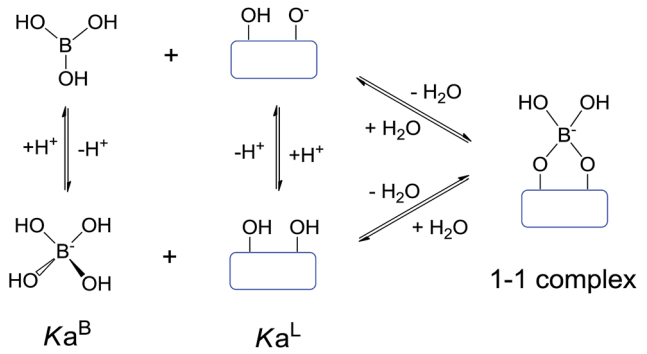

Fig. 8 Equilibrium and the 1–1 complex formation in aqueous solutions of borax and HPG.

derived from equilibrium constants and mass balances that the maximum amount of 1–1 crosslinking reaction products occurs at pH = $(pK_a^B + pK_a^L)/2$,[56–58] which will be beneficial for intermolecular 2–1 crosslinking reactions. In addition, larger amounts of NaOH are added to adjust the HPG solution to pH 12 and 13. And another possible situation is that the large number of Na^+ shields the electrostatic repulsion among the ionic groups of the HPG chains, which leads to the transformation from extension to coil for the HPG chain conformation, which hinders the intermolecular 2–1 crosslinking reactions.[59] So there is a maximum molecular weight of cross-linked gel with the increase of pH, and a maximum of T_{max} exists at pH 11. In degradation of the cross-linked gel, thermal oxidative action decreases because the redox potential of O_2 decreases and thermal alkaline hydrolysis is enhanced with increasing pH.[46–48] The different change trend of molecular weight of the cross-linked gel, thermal oxidative degradation, and thermal hydrolysis makes relatively complex changes of $T_{max}(\eta_0, t_0)$ with pH (Fig. 6b). At pH 7–9, $T_{max}(\eta_0, t_0)$ increases with pH mainly because of the increase of the molecular weight of cross-linked gel. At pH 9–11, thermal alkaline hydrolysis is enhanced meanwhile thermal oxidative action decreases and molecular weight increases, which results in little change in $T_{max}(\eta_0, t_0)$ with increasing pH. At pH 11–13, $T_{max}(\eta_0, t_0)$ continually increases with pH mainly because of the significant reduction of the thermal oxidative action.

5. Conclusions

In this work, a simple and effective approach has been proposed to evaluate the temperature–resistance performance of fracturing fluid. The temperature–resistance performance can be characterized by measuring the maximum tolerance temperature $T_{max}(\eta_0, t_0)$. And $T_{max}(\eta_0, t_0)$ is determined by a step-by-step numerical search method starting from the upper limit temperature T_{max}. Based on this evaluation method, the effects of various factors including HPG concentration, $Na_2B_4O_7$ concentration and pH value on the crosslink and temperature–resistance properties of borate cross-linked hydroxypropyl guar gum fracturing fluid were investigated systematically. The crosslinking time t_c decreases with the increase of the HPG concentration or $Na_2B_4O_7$ concentration, because those chemicals bring more crosslinking sites and the chance of crosslinking reaction also increases. Whereas the crosslinking time t_c increases with pH, because the amount of borate ion increases with pH and the reaction rate constant of a borate ion with *cis*-OH pairs is much smaller than that of boric acid. Interestingly, the variation tendency of $T_{max}(\eta_0, t_0)$ is different from that of T_{max}. $T_{max}(\eta_0, t_0)$ gradually increases with the increase of the HPG/$Na_2B_4O_7$ concentration, whereas T_{max} increases significantly at low HPG or $Na_2B_4O_7$ concentration and is almost unchanged at high $Na_2B_4O_7$ concentration. With the increase of pH, the maximum of T_{max} is observed at pH 11 owing to an optimal equilibrium for the intermolecular crosslinking reaction. The complex effects of pH on crosslinking reactions and degradation reactions make relatively complex changes of $T_{max}(\eta_0, t_0)$ with pH, *viz.*, $T_{max}(\eta_0, t_0)$ increases at pH 7–9, changes slightly at pH 9–11, and continuously increases at pH 11–13. This study may provide a common method for evaluating the temperature–resistance performance of the fracturing fluid. Our results provide useful insights into the understanding of temperature–tolerance performance of borate cross-linked hydroxypropyl guar gum fracturing fluid, and advance the application to increase well productivity in fields.

Conflicts of interest

There are no conflicts to declare.

Acknowledgements

This work is supported by Open Fund of State Key Laboratory of Oil and Gas Reservoir Geology and Exploitation (PLN1302), the NSFC program of China (51574267), the Fundamental Research Funds for the Central Universities (15CX08003A), the Program for Changjiang Scholars and Innovative Research Team in University (IRT_14R58) and the National Science Fund for Distinguished Young Scholars (51425406).

Notes and references

1 M. J. Economides and K. G. Nolte, *Reservoir Stimulation*, John Wiley and Sons, Ltd, New York, 3rd edn, 2000.
2 R. Barati and J. T. Liang, *J. Appl. Polym. Sci.*, 2014, **131**, 318–323.
3 G. A. Al-Muntasheri, *SPE Prod. Oper.*, 2014, **29**, 243–260.
4 A. C. Barbati, J. Desroches, A. Robisson and G. H. Mckinley, *Annu. Rev. Chem. Biomol. Eng.*, 2016, **7**, 415–453.
5 H. C. Lau, H. Li and S. Huang, *Energy Fuels*, 2017, **31**, 4588–4602.
6 P. C. Harris, *J. Pet. Technol.*, 1993, **45**, 264–269.
7 H. Quan, Z. Li and Z. Huang, *RSC Adv.*, 2016, **6**, 49281–49288.
8 Y. Liu and H. A. Li, *SPE Prod. Oper.*, 2016, **31**, 325–336.
9 Q. Jiang, G. Jiang, C. Wang, Q. Zhu, L. Yang, L. Wang, X. Zhang and C. Liu, *Paper SPE 180595 presented in part at the IADC/SPE Asia Pacific Drilling Technology Conference*, Singapore, 2016, DOI: 10.2118/180595-MS.

10 K. E. Friehauf and M. M. Sharma, *Paper SPE 124361 presented in part at the 2009 SPE Annual Technical Conference and Exhibition*, New Orleans, Louisiana, USA, 2009, DOI: 10.2118/124361-MS.
11 Q. Lv, Z. Li, B. Li, S. Li and Q. Sun, *Ind. Eng. Chem. Res.*, 2015, **54**, 9456–9477.
12 X. Sun, X. Liang, S. Wang and Y. Lu, *J. Pet. Sci. Eng.*, 2014, **119**, 104–111.
13 T. Huang and J. B. Crews, *SPE Prod. Oper.*, 2007, **24**, 60–65.
14 Z. Yan, C. Dai, M. Zhao, Y. Sun and G. Zhao, *J. Ind. Eng. Chem.*, 2016, **37**, 115–122.
15 X. P. Wu, Y. N. Wu, S. Yang, M. W. Zhao, M. W. Gao, H. Li and C. L. Dai, *Soft Matter*, 2016, **12**, 4549–4556.
16 A. Baruah, D. S. Shekhawat, A. K. Pathak and K. Ojha, *J. Pet. Sci. Eng.*, 2016, **146**, 340–349.
17 Y. Lu, F. Yang, Z. Ge, S. Wang and Q. Wang, *J. Nat. Gas Sci. Eng.*, 2015, **27**, 1649–1656.
18 W. Kang, P. Wang, H. Fan, H. Yang, C. Dai, X. Yin, Y. Zhao and S. Guo, *Soft Matter*, 2017, **13**, 1182–1189.
19 D. N. Harry, D. E. Putzig, M. Ralph, D. P. Tom and J. Peter, *Paper SPE 50731 presented in part at the 1999 SPE International Symposium on Oilfield Chemistry*, Houston, Texas, USA, 1999, DOI: 10.2118/50731-MS.
20 C. Lei and P. E. Clark, *SPE J.*, 2007, **12**, 316–321.
21 J. Maxey, Y. T. Hu, T. Kishore and D. Loveless, *Paper SPE 173726 presented in part at the SPE International Symposium on Oilfield Chemistry*, The Woodlands, Texas, USA, 2015, DOI: 10.2118/173726-MS.
22 S. Trabelsi and S. Kakadjian, *Paper SPE 164486, presented in part at the 2013 SPE Production and Operations Symposium*, Oklahoma City, 2013, DOI: 10.2118/164486-MS.
23 G. P. Funkhouser, J. Holtsclaw and J. Blevins, *Paper SPE 132173 presented in part at the SPE Deep Gas Conference and Exhibition*, Manama, Bahrain, 2010. SPE-132173-MS.
24 L. Song and Z. Yang, *Paper IPTC 18597 presented in part at the International Petroleum Technology Conference*, Bangkok, Thailand, 2016, DOI: 10.2118/18597-MS.
25 A. Baruah, A. K. Pathak and K. Ojha, *AIChE J.*, 2016, **62**, 2177–2187.
26 A. Baruah, A. K. Pathak and K. Ojha, *Chem. Eng. Sci.*, 2015, **131**, 146–154.
27 A. Baruah, A. K. Pathak and K. Ojha, *Ind. Eng. Chem. Res.*, 2015, **54**, 7640–7649.
28 J. Mao, X. Yang, D. Wang, Y. Li and J. Zhao, *RSC Adv.*, 2016, **6**, 88426–88432.
29 J. Holtsclaw and G. P. Funkhouser, *SPE Drill. Completion*, 2010, **25**, 555–563.
30 H. Quan, Z. Li and Z. Huang, *RSC Adv.*, 2016, **6**, 49281–49288.
31 K. Sokhanvarian, H. A. Nasr-El-Din and T. L. Harper, *Paper SPE 176837 presented in part at the SPE Asia Pacific Unconventional Resources Conference and Exhibition*, Brisbane, Australia, 2015, DOI: 10.2118/176837-MS.
32 R. A. Kalgaonkar and P. R. Patil, *Paper SPE 151890, presented in part at the SPE Oil and Gas India Conference and Exhibition*, Mumbai, India, 2012, DOI: 10.2118/151890-MS.
33 W. Xiaolan, Q. Qi, M. Scott, N. Jonathon, B. Kody and L. Neumann, *Paper SPE 73789 presented in part at the SPE International Symposium and Exhibition on Formation Damage Control*, Lafayette, Louisiana, 2002, DOI: 10.2118/73789-MS.
34 Y. Lv, Y. Feng, Z. Wang, A. Li, Q. Zhang, B. Huang, J. Zuo, Z. Ren and Y. Chen, *Paper SPE 184577 presented in part at the SPE International Conference on Oilfield Chemistry*, Montgomery, Texas, USA, 2017, DOI: 10.2118/184577-MS.
35 L. Wang, Z. Wen, C. Bo, Y. Lu and X. Qiu, *Paper SPE 26364 presented in part at the Offshore Technology Conference Asia*, Kuala Lumpur, Malaysia, 2016, OTC-26364-MS.
36 R. Kalgaonkar and P. Patil, *Paper SPE 152040 presented in part at the North Africa Technical Conference and Exhibition*, Cairo, Egypt, 2012, DOI: 10.2118/152040-MS.
37 A. M. Elsarawy, H. A. Nasr-El-Din and K. E. Cawiezel, *Paper SPE 180215 presented in part at the SPE Low Perm Symposium*, Denver, Colorado, USA, 2016, DOI: 10.2118/180215-MS.
38 H. M. Fan, Z. X. Wang, H. J. Fan, H. G. Zhou, J. Q. Zuo, K. Chen, Z. L. Wang, W. L. Kang and C. L. Dai, *J. China Univ. Pet., Ed. Nat. Sci.*, 2017, **41**, 160–166.
39 B. L. Chen, *Theory and Algorithms of Optimization*, Tsinghua University Press, Beijing, 2005.
40 Q. Li, Z. X. Wang, L. Y. Shen, Y. J. Wang and X. Y. Li, *Drill. Fluid Completion Fluid*, 2016, **33**, 57–62.
41 Cn-Sy, SY/T 6376-2008, *General technical specifications of fracturing fluids[s]*, National Development and Reform Commission, China, 2008.
42 P. C. Harris and A. Sabhapondit, *Paper SPE 120029 presented in part at the 2009 SPE Middle East Oil and Gas Show and Conference*, Bahrain, Bahrain, 2009, DOI: 10.2118/120029-MS.
43 M. Rietjens and P. A. Steenbergen, *Eur. J. Inorg. Chem.*, 2005, **2005**, 1162–1174.
44 I. Teraoka, *Polymer Solutions: An Introduction to Physical Properties*, 2002.
45 O. Bobleter, *ChemInform*, 2010, **29**, 893–936.
46 V. Soldi, in *Polysaccharides: Structural Diversity and Functional Versatility*, ed. Dumitriu, CRC Press, London, UK, 2nd edn, 2004, ch. 14, pp. 395–409.
47 R. Kivelä, T. Sontag-Strohm, J. Loponen, P. Tuomainen and L. Nyström, *Carbohydr. Polym.*, 2011, **85**, 645–652.
48 K. Dusek and M. Duskova-Smrckova, *Prog. Polym. Sci.*, 2000, **25**, 1215–1260.
49 J. Q. Jiang, B. Qi, M. Lepage and Y. Zhao, *Macromolecules*, 2007, **40**, 790–792.
50 J. A. Peters, *Coord. Chem. Rev.*, 2014, **268**, 1–22.
51 M. Bishop, N. Shahid, J. Yang and A. R. Barron, *Dalton Trans.*, 2004, 2621–2634.
52 S. Iwatsuki, S. Nakajima, M. Inamo, H. D. Takagi and K. Ishihara, *Inorg. Chem.*, 2007, **46**, 354–356.
53 Y. Yamamoto, T. Matsumura, N. Takao, H. Yamagishi, M. Takahashi, S. Iwatsuki and K. Ishihara, *Inorg. Chim. Acta*, 2005, **358**, 3355–3361.
54 E. Watanabe, J. Fujii, K. Kojima, S. Iwatsuki, M. Inamo, H. D. Takagi and K. Ishihara, *Inorg. Chem. Commun.*, 2010, **13**, 1406–1409.

55 H. Monajemi, M. H. Cheah, V. S. Lee, S. M. Zain and A. T. W. A. Wan, *RSC Adv.*, 2014, **4**, 10505–10513.
56 M. V. Duin, J. A. Peters, A. P. G. Kieboom and H. V. Bekkum, *Tetrahedron*, 1984, **40**, 2901–2911.
57 J. Yan, G. Springsteen, S. Deeter and B. Wang, *Tetrahedron*, 2004, **60**, 11205–11209.
58 M. A. Martínez-Aguirre, R. Villamil-Ramos, J. A. Guerrero-Alvarez and A. K. Yatsimirsky, *J. Org. Chem.*, 2013, **78**, 4674–4684.
59 S. Wang, H. Tang, J. Guo and K. Wang, *Carbohydr. Polym.*, 2016, **147**, 455–463.